



PII S0016-7037(02)01083-9

Iron oxidation state of a 2.45-Byr-old paleosol developed on mafic volcanics

SATOSHI UTSUNOMIYA,^{1,†} TAKASHI MURAKAMI,¹ MASAMI NAKADA,^{2,*} and TAKESHI KASAMA^{1,‡}

¹Department of Earth and Planetary Science, The University of Tokyo, 7-3-1 Hongo, Tokyo 113-0033, Japan

²Japan Atomic Energy Research Institute, Tokai-mura, Ibaraki-ken 319-1195, Japan

(Received March 12, 2002; accepted in revised form July 29, 2002)

Abstract—The 2.45-Byr-old weathering profile developed on early Proterozoic mafic volcanics located near Cooper Lake, Ontario, Canada, was examined geochemically and mineralogically for a better understanding of the atmospheric oxygen evolution. Ferrous to ferric ion, Fe(II) and Fe(III), respectively, ratios of the bulk rock samples were analyzed by Mössbauer spectrometry. The total Fe (Fe(T)) and Fe(II) concentrations decrease from 12.0 and 11.2 wt.% to 1.85 and 0.89 wt.%, respectively, from the bottom to the top of the weathering profile. The Fe(T) and Fe(II) concentrations normalized to Ti and Zr, as well as the Fe(II)/Fe(III) ratio of raw data, linearly decrease with depth toward the top, while the Fe(III) concentration remains nearly constant throughout the profile. The linear decrease of Fe(II), accompanied by the nearly constant distribution of Fe(III), is difficult to be explained by the scenario of oxidizing weathering and subsequent reducing hydrothermal alteration. The behaviors of Fe(II) and Fe(III) can be simply explained by anoxic weathering. The anoxic weathering suggests that the 2.45-Ga atmosphere was anoxic. The slight increase of Fe/(Fe+Mg) in the octahedral sites of chlorite toward the top and no Ce anomaly in the REE patterns are also consistent with anoxic weathering. Copyright © 2003 Elsevier Science Ltd

1. INTRODUCTION

Two atmospheric components, CO₂ and O₂, have played an important role in water-rock interactions on the Earth's surface in terms of acidity and oxidization, respectively. The CO₂ and O₂ concentrations have changed drastically through the Earth's history. In the Archean, the CO₂ concentration was 10² to 10³ times higher than at present (Kasting, 1987, 1993). On the other hand, O₂ was 10⁻³ times lower or nearly absent in the early atmosphere (Kasting and Ackerman, 1986) and began to increase around 2.4 Ga (Kasting, 1991). Because the two components were closely related to weathering, some vestiges of water-rock-atmosphere interactions must be preserved in ancient weathering profiles called "paleosols" (Holland, 1984).

The evolution of CO₂ has been established based on several factors such as solar luminosity and greenhouse effect that restrict the CO₂ level (Kasting, 1993). However, there are not enough global factors to calculate the O₂ concentration in the Precambrian atmosphere (Kasting, 1993). Thus, some geological evidences are necessary to establish O₂ evolution. Indeed, paleosol studies have provided some constraints of O₂ level (e.g., Holland, 1984; Grandstaff et al., 1986; Holland and Zbinden, 1988; Pinto and Holland, 1988; Holland et al., 1989; Holland and Beukes, 1990; Macfarlane et al., 1994; Prasad and Roscoe, 1996). From investigation of paleosols, the O₂ level in the atmosphere is considered to have changed dramatically between 2.2 and 2.0 Ga from < 0.002 atm to > 0.03 atm (Holland and Rye, 1997; Rye and Holland, 1998). The evaluation is mainly based on Fe retention in paleosols, because Fe

is the dominant element consuming O₂ during the weathering of igneous rocks. The maximum O₂ level is estimated by the following equation:

$$H_{O_2}P_{O_2}/H_{CO_2}P_{CO_2} < M_{O_2}/8M_{CO_2} \quad (1)$$

where H_i is the Henry's constant, P_i the partial pressure of gas, and M_i the difference of the concentration of species i between the parent rock and the most intensely weathered soil (M_{O₂} for FeO and M_{CO₂} for CaO, MgO, Na₂O, K₂O, and MnO) (Rye and Holland, 1998). Maximum P_{CO₂} is necessary to obtain maximum P_{O₂} in this equation. For instance, Rye et al., (1995) calculated the maximum P_{O₂} to be 5 × 10⁻⁴ atm for several Elliot Lake paleosols based on the maximum P_{CO₂} at ~2.5 Ga. They estimated the maximum P_{CO₂} based on greenalite-siderite equilibrium, assuming that the secondary mineral was greenalite during the paleo-weathering.

In the above discussions on the relationships between atmospheric O₂ level and paleosol, there are two important ideas: (1) Iron distribution in a paleosol profile is the main factor that determines the amount of consumed O₂ and (2) the equilibrium of secondary minerals containing Fe determines the maximum levels of CO₂ and thus O₂, finally.

The present study examines a 2.45-Ga paleosol containing high Fe concentration, which, therefore, can provide information on the behavior of Fe during 2.45-Ga weathering. We discuss atmospheric O₂ based on the distribution of ferrous and ferric ion (hereafter referred to as Fe(II) and Fe(III), respectively) determined by Mössbauer spectrometry.

2. SAMPLES

The research area is located near Boundary Lake, which lies ~1-km north of Cooper Lake and is ~50-km east of Sault Ste. Marie, Ontario, Canada (Fig. 1). Detailed geology of the locality is given by G.-Farrow and Mossman (1988) and Robertson (1970, 1981). According to the description of geology by

* Author to whom correspondence should be addressed (murakami@eps.s.u-tokyo.ac.jp).

† Present address: Nuclear Engineering and Radiological Sciences, College of Engineering, University of Michigan, Ann Arbor, MI 48109-2104, USA.

‡ Present address: Institut für Mineralogie, Universität Muenster, D-48149 Muenster, Germany.

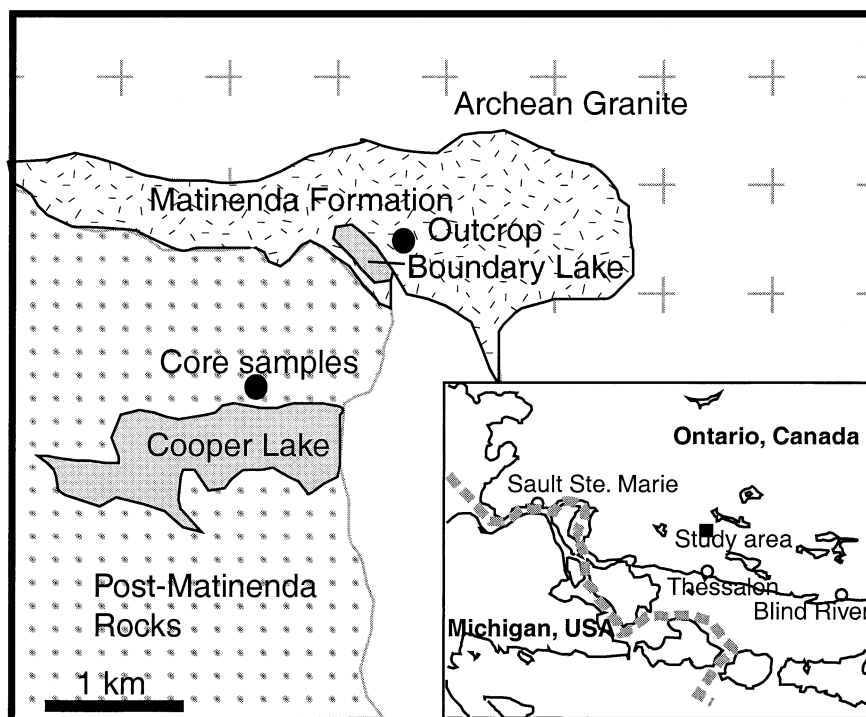


Fig. 1. Location of the paleosol of the present study (modified from Sutton and Maynard, 1993). The Thessalon mafic volcanics lies below the Matinenda Formation at the outcrop.

Prasad et al., (1993) and Bennett et al. (1997), the Thessalon Formation is part of volcanic rocks of the Elliot Lake Group, which are the only known volcanic rocks of the Huronian Supergroup. The Thessalon Formation consists of tholeiitic mafic flows. The mineral assemblage indicates subgreenschist-to-greenschist facies metamorphism, which might have occurred during the Penokean Orogeny ~ 1.85 Ga (Card, 1978; Prasad and Roscoe, 1991). In general, the Thessalon Formation overlies the Livingstone Creek Formation, an upper fine- to medium-grained arkose and a lower, clast-supported polymictic conglomerate. At the present sampling location, the width of the exposed Livingstone Creek sandstone is ~ 5 m, and the sandstone is adjacent to a 10-m-wide exposed portion of the Thessalon Formation. Depth of the exposure is 5 to 6 m for both formations. The Matinenda Formation of the upper Elliot Group unconformably overlies both the Livingstone Creek Formation and the Thessalon Formation. The Matinenda Formation is exposed to a width of a few meters and a depth of several tens of centimeters. The Matinenda Formation consists of quartz and feldspar grain conglomerates in a matrix of sericite, which is an important host of uranium deposits.

The present weathering profile is developed on the Thessalon mafic volcanics and is unconformably overlain by the Matinenda quartz-pebble conglomerate. The weathering profile was first described by Sutton and Maynard (1993) and was classified as a "definite paleosol" by Rye and Holland (1998). The paleosol was formed between 2.7 and 2.4 Ga based on the age of the youngest Archean basement at 2665 (+1.6/−1.4) Ma (Sutton and Maynard, 1993; Prasad and Roscoe, 1996) and that of the overlying Matinenda Formation, which is nearly coeval with the Coppercliff Formation rhyolite at 2450 (+25/−10) Ma

(Krogh et al., 1984). Rye and Holland (1998) suggested ~ 2450 Ma for the formation age of the paleosol. The paleosol was also subjected to very low metamorphism at ~ 1.85 Ga (Card, 1978).

Samples collected and used for the present study were from the Thessalon mafic volcanics and the Matinenda Formation (Table 1). Depths in Table 1 represent the vertical distance from the unconformity plane to a sampling point; the samples with negative values were from the Thessalon mafic volcanics, and the samples with positive values from the Matinenda Formation. The sample at -5.3 m was free of sericite and was considered to be relatively unweathered. We did not use samples near the boundaries between the Thessalon and Livingstone Creek Formations, because the samples near the boundaries were rich in quartz probably from the Livingstone Creek Formation. Drill cores from Cooper Lake (Imperial Oil drill hole No.68-2) that are believed to be the same as the Thessalon mafic rock (Sutton and Maynard, 1993) were used as reference for the present study (cores 1271 and 1338). The core samples did not contain sericite, and the sample was considered to be relatively unweathered.

3. MATERIAL AND METHODS

About 100 g of each rock sample was powdered and homogeneously mixed for X-ray fluorescence spectrometry (XRF), inductively coupled plasma mass spectrometry (ICP-MS), and X-ray diffraction (XRD) analysis. Major elements of the bulk samples were analyzed by XRF (Philips PW 1480). A sample was mixed with lithium borate, and the mixture was melted at $\sim 1300^\circ\text{C}$ and quenched, which provided a platy glass for XRF measurement. For some trace elements, a disk sample after pressing powder was used and analyzed by XRF. Refer to Yoshida and Takahashi (1997) for the quality and accuracy of the present XRF data. ICP-MS (Hewlett Packard HP-4500) was used to analyze rare

Table 1. Bulk chemical compositions of major elements, Fe(II), and Fe(III) (wt%) and Fe(II)/Fe(III) ratios (a), trace element concentrations (ppm) (b) and rare earth element concentrations (ppm) (c).

(a) Depth (m)	SiO ₂	TiO ₂	Al ₂ O ₃	Fe ₂ O ₃ *	MnO	MgO	CaO	Na ₂ O	K ₂ O	P ₂ O ₅	Fe(II)	Fe(III)	Fe(II)/Fe(III)
+0.25	85.0	0.15	8.57	1.23	ND**	0.18	0.13	ND	3.66	0.03			
+0.05	87.3	0.09	7.59	0.90	ND	0.19	0.14	ND	3.23	0.04			
-0.25	55.9	1.95	25.9	2.64	ND	1.10	0.13	ND	9.24	0.05	0.89	0.96	0.93
-0.50	58.0	1.79	23.6	3.09	ND	1.23	0.21	ND	8.58	0.11	0.94	1.22	0.77
-1.4	52.7	2.09	21.9	8.98	0.04	2.43	0.46	ND	6.97	0.28	4.69	1.59	2.96
-2.0	53.4	1.79	21.6	9.18	0.01	2.35	0.44	ND	6.95	0.27	5.25	1.17	4.49
-3.0	52.8	1.92	20.3	11.4	0.03	2.88	0.47	ND	5.92	0.29	6.97	1.01	6.87
-4.0	47.9	1.92	19.1	16.9	0.05	4.40	0.44	ND	4.28	0.26	10.7	1.16	9.23
-5.3	54.1	1.38	14.9	17.1	0.09	4.48	1.03	2.62	0.97	0.18	11.2	0.75	15.0
Core1271	48.4	1.25	18.0	17.0	0.09	4.86	0.81	3.80	2.42	0.17			
Core1338	43.1	1.58	16.4	22.0	0.11	7.54	1.60	2.75	0.57	0.21			

(b) Depth (m)	Ba	Cr	Nb	Ni	Pb	Rb	Sr	Th	Y	Zr
+0.25	553	26	3	9	4	120	23	6	5	73
+0.05	528	25	1	8	3	109	24	3	8	54
-0.25	717	57	8	24	2	327	17	6	62	247
-0.50	705	83	7	28	3	327	17	6	25	215
-1.4	519	66	6	49	2	290	25	6	44	230
-2.0	548	52	7	58	5	283	20	6	45	203
-3.0	493	57	8	51	2	244	17	7	51	213
-4.0	339	64	6	60	2	180	17	6	34	198
-5.3	61	51	4	54	2	20	44	5	22	145
Core1271	277	100	3	59	3	134	144	2	23	106
Core1338	91	109	4	75	0	22	95	3	27	138

(c) Depth (m)	La	Ce	Pr	Nd	Sm	Eu	Gd	Tb	Dy	Ho	Er	Tm	Yb	Lu
+0.25	14.5	27.6	2.51	9.82	1.63	0.45	1.03	0.08	0.46	0.06	0.21	0.01	0.22	0.02
+0.05	12.6	24.6	2.31	9.23	1.55	0.42	1.06	0.09	0.58	0.09	0.28	0.02	0.25	0.02
-0.25	61.1	135	13.7	62.3	13.3	3.65	10.2	1.20	6.77	1.31	4.25	0.63	4.43	0.68
-0.50	9.77	24.8	2.65	11.9	2.78	0.89	3.01	0.46	3.16	0.63	1.96	0.26	1.87	0.26
-1.4	19.4	42.2	5.16	21.3	4.72	1.34	4.86	0.74	4.91	1.08	3.46	0.51	3.60	0.55
-2.0	48.6	110	11.2	49.7	10.5	2.73	8.52	1.06	5.86	1.19	3.53	0.50	3.45	0.52
-3.0	25.8	60.6	6.36	28.5	6.15	1.75	5.59	0.75	4.77	1.00	3.23	0.46	3.31	0.50
-4.0	10.3	25.8	2.78	12.9	3.22	0.95	3.49	0.55	3.84	0.83	2.74	0.40	2.90	0.44
-5.3	6.66	14.2	1.67	7.19	1.77	0.57	2.11	0.35	2.56	0.59	1.98	0.29	2.12	0.31
Core1271	7.15	15.8	1.95	8.64	2.30	0.77	2.80	0.48	3.35	0.72	2.25	0.31	2.13	0.31
Core1338	15.4	33.1	3.89	16.4	3.78	1.06	3.95	0.63	4.08	0.84	2.53	0.35	2.35	0.34

* All Fe is given as Fe₂O₃. ** ND represents "not detected".

earth elements (REEs). A solution for ICP-MS measurement was prepared by the following procedure: 1 g of powdered sample was dissolved in a perchloric and hydrofluoric acid solution; the solution was evaporated; the dried residuum was dissolved in a hydrochloric and nitric acid solution; and finally pure water was added to the solution to make 100 mL of a final solution. We did not find any residua in the final solutions.

Identification of major constituent minerals of the rocks was made by XRD (Rigaku RINT2000). Subjected to XRD were 2 g of each powder from the bulk samples. The 0.2 g of powder were placed on a sample holder without pressure to prevent preferential sorting of layer silicates. The amount of chlorite and sericite was estimated semiquantitatively by XRD. Sericite and chlorite were the only minerals that had peaks at 1.0 and 0.7 nm, respectively, among the major constituent minerals. The sample at -0.25 m was richest in sericite, and the sample at -5.3 m was richest in chlorite. Therefore, a ratio of 1.0-nm peak height of a sample to one at -0.25 m for sericite and a ratio of 0.7-nm peak height of a sample to one at -5.3 m for chlorite were calculated.

Fe(II)-to-Fe(III) ratios in the bulk samples were determined by Mössbauer spectrometry. A Mössbauer spectrometer (Laboratory Equipment VT-6000) with a ⁵⁷Co(Rh) source was operated using

constant acceleration motion. Mössbauer spectra were obtained in the transmission geometry at room temperature. The Doppler velocity was calibrated using α -Fe. For each sample, several thin sections measuring 2 × 2 cm × ~100- μ m thick were prepared and stacked. The number of stacked thin sections varied depending on the relative intensity of absorption. Each Mössbauer spectrum was deconvoluted by profile fitting. We found only two Fe oxidation states, Fe(II) and Fe(III), in all spectra. One example (sample at -1.5-m deep) of a Mössbauer spectrum, along with its deconvoluted Fe(II) and Fe(III) profiles, is shown in Figure 2. The Fe(II)-to-Fe(III) mole ratios were derived from the intensities of deconvoluted profiles ascribed to the two respective ions.

Microscale observation and semiquantitative analysis of individual minerals were performed by field emission scanning electron microscopy with energy-dispersive X-ray spectrometry (FE-SEM + EDS) (Hitachi S-4500). Quantitative analysis of chlorite grains was carried out by SEM + EDS (JEOL JXA-840A) with standards.

4. RESULTS

Major mineral assemblages in the weathering profile are shown in Figure 3. The abundance of quartz did not change

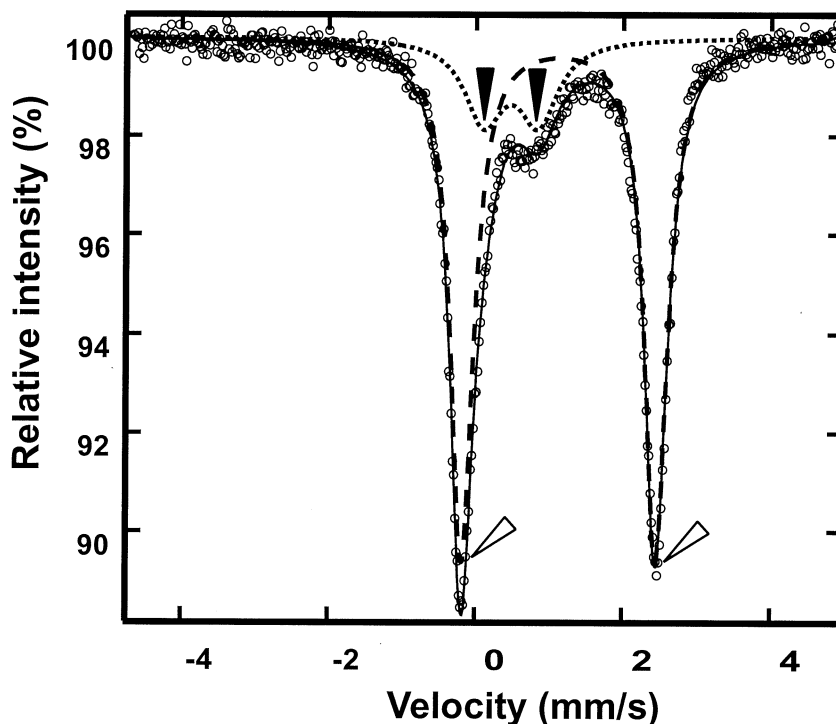


Fig. 2. Typical Mössbauer spectrum with deconvoluted Fe(II) and Fe(III) profiles (dashed and dotted curves, respectively). The sample at -1.5 m-deep was used. Black arrows show absorption peaks of Fe(III) and open arrows Fe(II). Open circles denote measured values.

significantly through the weathering profile. Albite was observed below -5.3 m. Chlorite occurred in the lower part, decreased gradually toward the top, and persisted up to -1.5 m. In contrast, sericite was not found in the lowest part (-5.3 m) and increased in the amount gradually toward the top. The increase of sericite toward the top corresponded to the increase in the K concentration in the bulk samples as discussed below. The minor minerals, ilmenite, rutile, pyrite, calcite, and barite, were observed. Amygdules, a characteristic texture of the parent rock and original vesicles, were filled with chlorite that was gradually replaced by sericite, and they were rimmed by quartz toward the top.

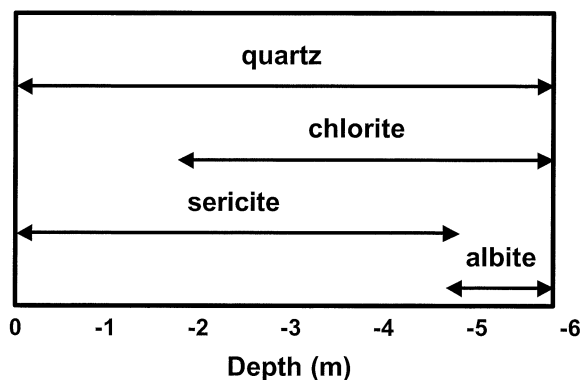


Fig. 3. Schematic illustration of the transition of major mineral assemblages in the weathering profile.

The chemical composition of the bulk samples is given in Table 1, and variations of major elements in the weathering profile are shown in Figure 4. The silica concentration was nearly constant at ~ 54 wt.% ($\pm 10\%$) throughout the weathering profile. Aluminum tended to increase slightly toward the top. Sodium was present only at a depth of -5.3 m (Table 1), which corresponded to the presence of albit. Potassium increased toward the top, which was related to the increase in abundance of sericite. The K increase is due to postweathering K-metasomatism (e.g., Rainbird et al., 1990; Nesbitt, 1992). Magnesium and Ca decreased toward the top. The drastic decrease of Mg, Ca, and Na in the upper part is common in paleosols (Nesbitt, 1992; Rye and Holland, 1998) as well as in modern profiles (Nesbitt et al., 1980). Iron decreased toward the top. The Fe decrease is in contrast with constant Fe concentration through modern, oxidizing weathering profiles, where dissolved Fe(II) is oxidized to Fe(III) and remains as Fe(III) oxides in the profile. The decrease of Mg and Fe is largely due to the decrease in abundance of chlorite. The Ti concentration remained almost constant through the weathering profile except at -5.3 m, whereas Zr increased slightly toward the top (Table 1). The chemical compositions of drill-cores 1271 and 1338 from Cooper Lake (Table 1; Fig. 4) were similar to the chemical composition of the sample at -5.3 -m deep. The small difference in composition between the drill-core samples and the sample at -5.3 m is probably due to a local difference in composition; the distance between the two rock samples is ~ 1.5 km.

Aluminum, Ti, and Zr are considered to be relatively immo-

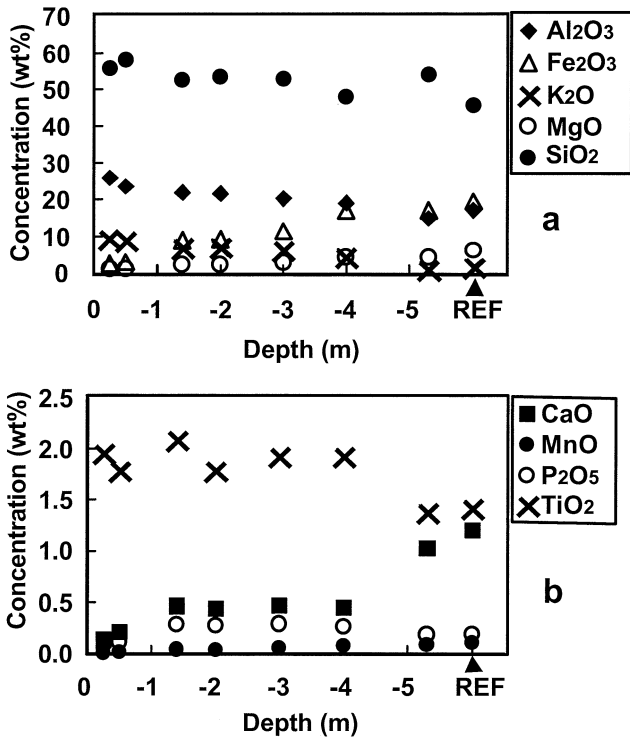


Fig. 4. Variations of major elements in the weathering profile. All Fe is given as Fe₂O₃. REF is the average composition of the core samples.

ble during weathering (e.g., Rye and Holland, 1998). Variations of Ti/Al, Zr/Ti, and Al/Zr against depth are shown in Figure 5. The ratios were approximately constant through the weathering profile. The deviations of the ratios were about $\pm 14\%$, $\pm 10\%$, and $\pm 7\%$ for Ti/Al, Zr/Ti, and Al/Zr, respectively. The Ti/Al and Zr/Ti ratios slightly decreased and increased, respectively, at the upper part, which are related to the constant Ti concentration and the slight increase of Al and Zr (Table 1).

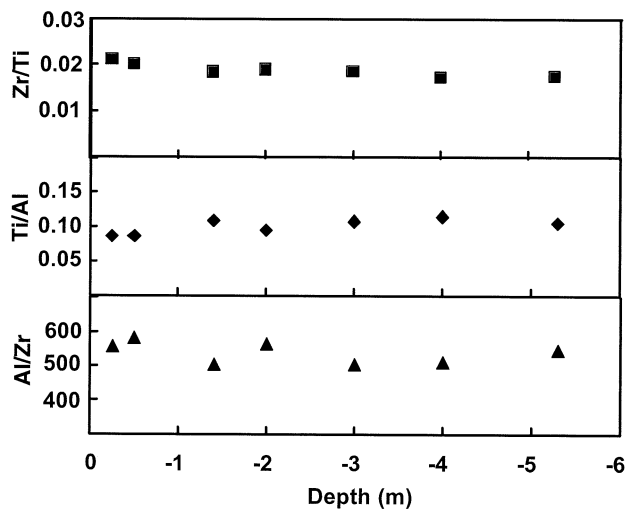


Fig. 5. Ratios in element percent of immobile elements, Ti, Al, and Zr, at various sampling depths.

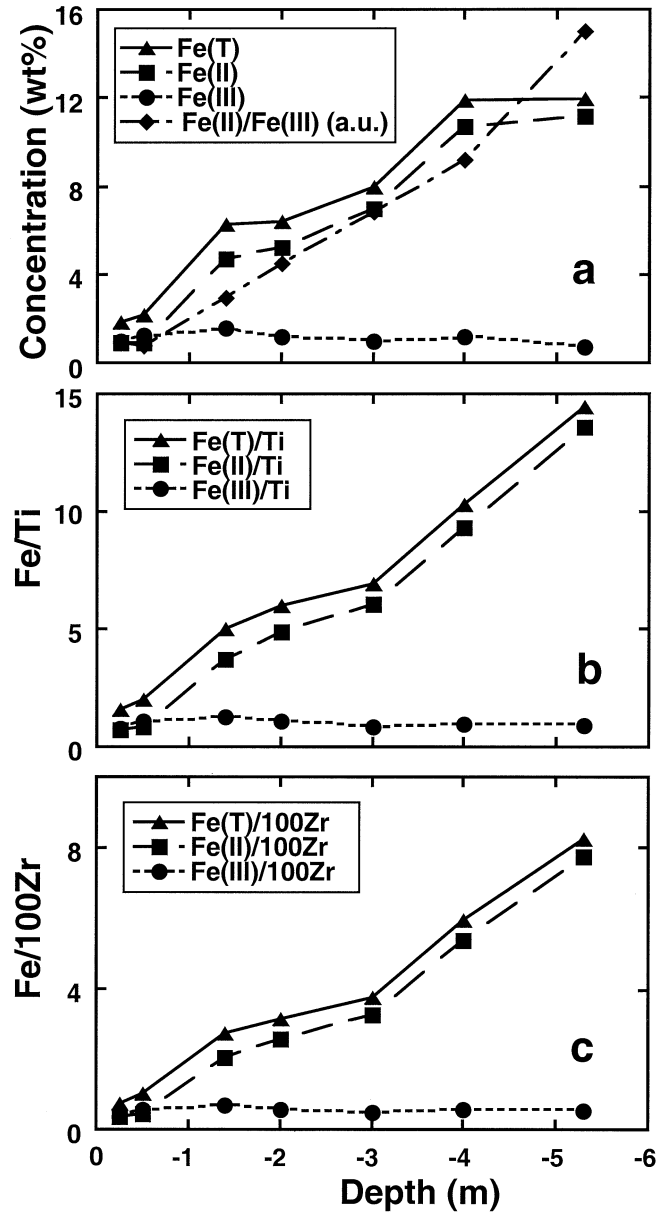


Fig. 6. Variations of total Fe (Fe(T)), Fe(II), and Fe(III) concentrations (wt.%) and that of Fe(II)/Fe(III) (arbitrary unit) (a) and variations of Fe(T), Fe(II), and Fe(III) normalized to Ti (b) and Zr (c) with depth. 100Zr denotes that a Zr concentration is multiplied by 100.

Variations of total Fe (hereafter, Fe(T)), Fe(II), and Fe(III) concentrations in the weathering profile are shown in Figure 6, along with that of the Fe(II)-to-Fe(III) ratios. Fe(III) was constant throughout the profile. In contrast, Fe(T) and Fe(II) concentrations decreased from 12.0 and 11.2 wt.% to 1.85 and 0.89 wt.%, respectively, from the bottom to top of the weathering profile. The uniform decrease was more distinct in the Fe(II)-to-Fe(III) ratios. Such linear decreases of Fe(II)/Fe(III) have never been reported previously for pre-2.0-Ga paleosols developed on basaltic rocks (Holland and Zbinden, 1988; Macfarlane et al., 1994). Fe(T), Fe(II), and Fe(III) normalized to Ti and Zr (Figs. 6b and 6c, respectively) exhibited the variations more

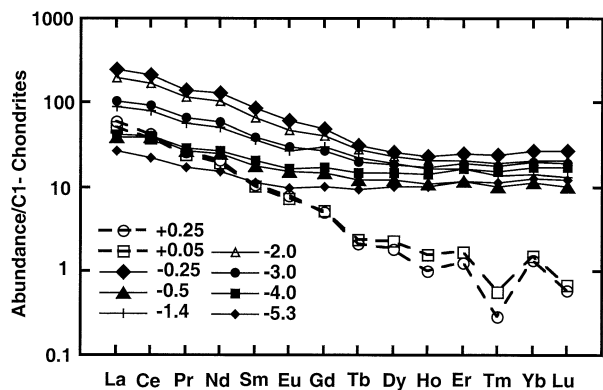


Fig. 7. REE patterns at different depths and those of two samples of the Matinenda Formation. REE concentrations are normalized to those of C1 chondrites (Palme et al., 1981).

clearly, that is, Fe(T) and Fe(II) linearly decreased toward the top of the profile, and Fe(III) was nearly constant throughout the profile. The linear decrease of the Fe(II) variations normalized to Ti and Zr is almost the same as that of Fe(II)/Fe(III) in Figure 6a. Therefore, slight deviations from linearity appearing in the Fe(T) and Fe(II) variations of the raw data (Fig. 6a) can result from heterogeneous Fe distribution in the original rock and/or heterogeneous weathering, even at the same depth. Compaction of the weathering profile and changes associated with later geological events, if any, did not change the depth variation of Fe(T), Fe(II), and Fe(III).

REE patterns of the samples from the weathering profile and Matinenda Formation (Table 1), normalized to C1 chondrite REEs (Palme et al., 1981), are illustrated in Figure 7. The REE patterns in the weathering profile were similar to one another, but they did not show significant anomalies of any elements through the profile. All REE concentrations gradually increased toward the top except for those of the samples at -0.5 and -1.4 m. In contrast, the REE patterns of the Matinenda samples were different from those in the weathering profile, which indicates different origins of REEs between the two different groups of samples.

Figure 8 shows variation of Fe/(Fe+Mg) mole ratios against

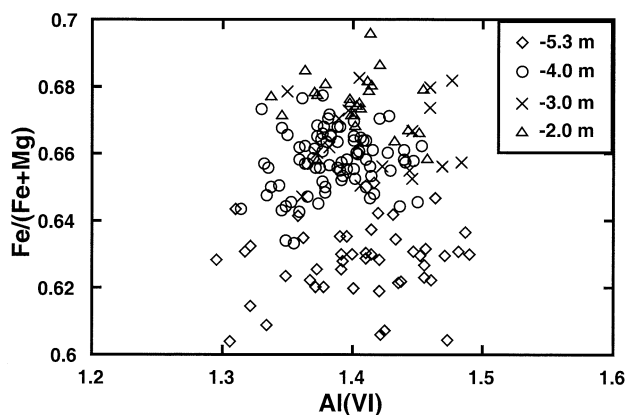


Fig. 8. Ratios of Fe/(Fe+Mg) against Al cations in the octahedral sites in chlorite based on $O_{10}(OH)_8$.

octahedral Al cation number in matrix chlorite at depths of -2.0 , -3.0 , -4.0 , and -5.3 m. Although the data were scattered even at one depth, there is a tendency for the value of Fe/(Fe+Mg) to increase slightly toward the top of the weathering profile. That is, as the depth decreased, matrix chlorite contained more Fe than Mg. On the contrary, the Fe and Mg concentrations in the bulk samples decreased almost in the same ratio (Table 1; Fig. 4).

5. DISCUSSION

Rye and Holland (1998) reviewed more than 50 reported paleosols and classified them based on five criteria. The paleosol used for the present study (referred to as Cooper Lake paleosol in their paper) has been classed as a “definite paleosol.” Indeed, our data show that the Cooper Lake paleosol meets the five criteria. The decrease of major alkalis and alkaline earths, except for K, toward the top of the weathering profile is characteristic of weathering (e.g., Middelburg et al., 1988). The ratios of the three immobile elements, Ti/Al, Zr/Ti, and Al/Zr, are nearly constant ($\pm 14\%$) throughout the weathering profile, suggesting that the Cooper Lake paleosol has not been disturbed significantly and is a well-preserved weathering profile, at least chemically. Therefore, the Cooper Lake paleosol is one of the best samples for examining the chemical change of a rock during early Proterozoic weathering.

To evaluate a degree of alteration in the weathering profile, CIA (chemical index of alteration; Nesbitt and Young, 1982) and CIW (chemical index of weathering; Harnois, 1988) values were calculated (Fig. 9):

$$\text{CIA} = \frac{\text{Al}_2\text{O}_3}{(\text{Al}_2\text{O}_3 + \text{CaO}^* + \text{Na}_2\text{O} + \text{K}_2\text{O})} \times 100 \quad (2)$$

and

$$\text{CIW} = \frac{\text{Al}_2\text{O}_3}{(\text{Al}_2\text{O}_3 + \text{CaO}^* + \text{Na}_2\text{O})} \times 100, \quad (3)$$

where the oxides are in moles and CaO^* represents CaO only in silicate minerals. The CIA and CIW values of fresh basalt of Mt. Roe are ~ 38 to 47% and 41 to 55%, respectively (Macfarlane et al., 1994). The core samples and the sample at -5.3 m have higher values (Fig. 9) and are not fresh; these samples are relatively unweathered compared to the samples at shallower depths. The CIA variation reveals a gradual decrease from -4.0 m to the top (Fig. 9). This reverse trend at the upper portion is attributed to postweathering K-metasomatism that added more K at the top of the profile (Rainbird et al., 1990; Nesbitt, 1992). Indeed, the CIW values, which do not include a contribution from K, indicate that the samples at -4.0 m and shallower are intensely weathered (Fig. 9).

An A-CN-K ternary diagram (Al, Ca+Na, and K in molar proportions) and an A-CNK-FM diagram (Al, Ca+Na+K, and Fe+Mg in molar proportions) are shown in Figure 10 to examine the weathering trend and the effect of K-metasomatism on the weathering profile (Nesbitt, 1992; Fedo et al., 1995). The data of fresh basalt of Mt. Roe (Macfarlane et al., 1994) are also plotted in Figure 10 for comparison. The A-CN-K diagram reveals that little K was introduced at -5.3 m deep. The K addition increases from a depth of -4.0 m to the top of the profile, which changes the apparent weathering trend

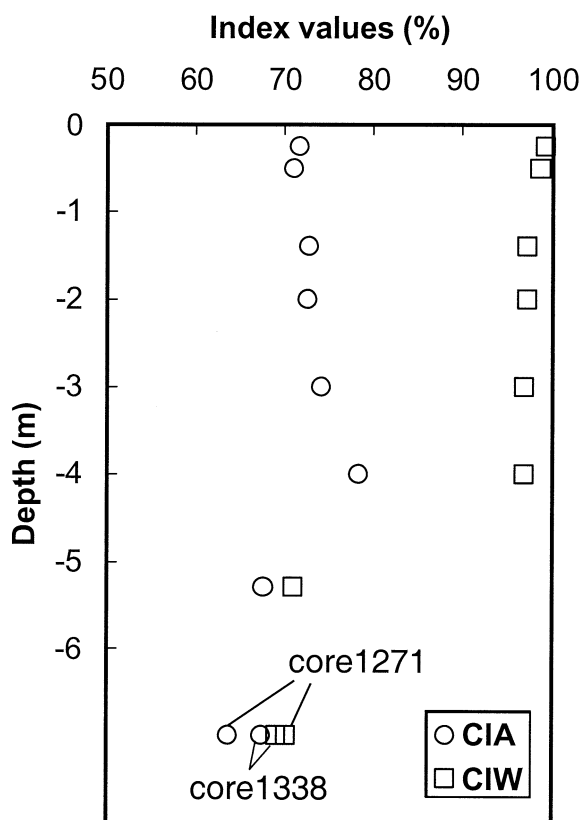


Fig. 9. Chemical index of alteration (CIA) and chemical index of weathering (CIW).

as shown by the dotted (Nesbitt, 1992) and solid lines. Although we do not have the data of a fresh parent rock, the difference in weathering trend is distinct between modern, oxic weathering (Nesbitt, 1992) and early Proterozoic weathering (dotted and solid lines, respectively, in the A-CN-K-FM diagram), which mainly results from the Fe loss in the upper profile.

The variations of Fe in the weathering profile are essentially the same whether the raw data or the normalized data based on Ti or Zr is used; the Fe(II)/Fe(III), Fe(II)/Ti, and Fe(II)/Zr ratios decrease almost linearly toward the top, and the Fe(III) concentration, Fe(III)/Ti, and Fe(III)/Zr are nearly constant throughout the profile (Fig. 6). The decrease of the Fe(T) and Fe(II) concentrations can be well interpreted as a result of anoxic weathering. However, Ohmoto (1996, 1997) insisted that the atmosphere through late Archean to early Proterozoic was oxic enough to precipitate Fe(III) minerals and that the decrease of the Fe(T) and Fe(II) concentrations occurred later as the result of hydrothermal alteration and/or organic acids, whereby Fe(III) was reduced to Fe(II) and then removed from the profile. The reduction of Fe(III) to Fe(II) in the weathering profile may require a large amount of a biomass. We have no evidence for the presence of a terrestrial biomass 2.45 Ga that could act as a reductant for Fe(III) (e.g., Pinto and Holland, 1988). We can therefore conclude that organic acids had little effect on the Fe(II) loss.

The abundance of chlorite corresponds proportionally to that

of Fe in the weathering profile and decreases toward the top (Figs. 3, 6). Because the sample at -5.3 -m deep is in the weathered zone as described above, the solution containing K must have reached the zone at -5.3 m and probably deeper. If the Fe loss occurred by reduction associated with the passage of the solution, it is unlikely that Fe in the upper profile was removed, while at the same time, most Fe in the lower profile remained. It is more likely that the solution formed chlorite at the expense of primary and/or secondary Fe(II)-bearing minerals. It is also likely that the homogeneous distribution of Fe(III) throughout the profile (Fig. 6) reflects the Fe(III) concentration of the parent rock. Thus, the Fe decrease toward the top is better explained by anoxic weathering rather than oxic weathering and subsequent reduction by hydrothermal solution.

The values of Fe/(Fe+Mg) in the octahedral sites of chlorite vary with depth and increase slightly toward the top of the weathering profile (Fig. 8). If the chlorites at different depths were formed from one primary Fe-bearing mineral such as biotite, one could expect similar Fe/(Fe+Mg) ratios of chlorites at different depths. The different ratios of Fe/(Fe+Mg) at different depths suggest that there were secondary Fe-bearing mineral(s) such as Fe-bearing smectite that had different Fe/Mg ratios from that of a primary Fe-bearing mineral. Such secondary Fe-bearing mineral(s), together with a primary Fe-bearing mineral, could have been a precursor of the chlorites. Therefore, the chloritization of the Cooper Lake paleosol was a postweathering event, not a preweathering event. The process described above is consistent with anoxic weathering.

The large difference in the REE patterns between the Cooper Lake paleosol and the Matinenda Formation (Fig. 7) indicates different origins of REEs between the two. Therefore, hydrothermal activities that could have affected both are excluded from the REE origin of the Cooper Lake paleosol. REEs are enriched toward the top of a weathering profile for modern weathering (e.g., Nesbitt, 1979). The general increase of REE toward the top (Fig. 6) is another evidence that the Cooper Lake paleosol was formed by weathering. Modern, oxidizing weathering oxidizes Ce^{3+} to Ce^{4+} and forms cerianite, CeO_2 (Braun et al., 1990, 1993), which causes different behavior of Ce from those of La and Nd in solution. The different behavior usually results in a Ce anomaly in REE patterns (Braun et al., 1990, 1993). Murakami et al. (2001) found Ce-rich rhabdophane, $(REE)PO_4$, in a 2.5-Ga Pronto paleosol and indicated that La, Ce, and Nd behaved the same in the solution, that is, Ce^{3+} remains as it is during anoxic weathering. They also showed no Ce anomaly throughout the weathering profile. Our REE patterns indicate no Ce anomaly, which is not inconsistent with anoxic weathering.

Acknowledgments—The authors are grateful to J. F. Banfield for useful discussion, to T. Tachikawa, H. Yoshida, and Y. Imazu for technical assistance, and to M. Hailstone at Ontario Geological Survey, who helped us while collecting samples. The authors are also grateful to N. Yanase and T. Ohnuki at the Japan Atomic Energy Research Institute, who kindly permitted us to use ICP-MS. R. C. Ewing at University of Michigan kindly allowed S.U. to complete this work at the current address. The authors also thank K. Traexler for reviewing an earlier version of this manuscript. The useful comments of H. D. Holland, L. R. Kump, and G. M. Young have greatly improved the quality of the paper. The electron microscopy was performed in the Electron Microbeam Analysis Facility for Mineralogy at the Department of Earth and Planetary Science, University of Tokyo. This work was partially

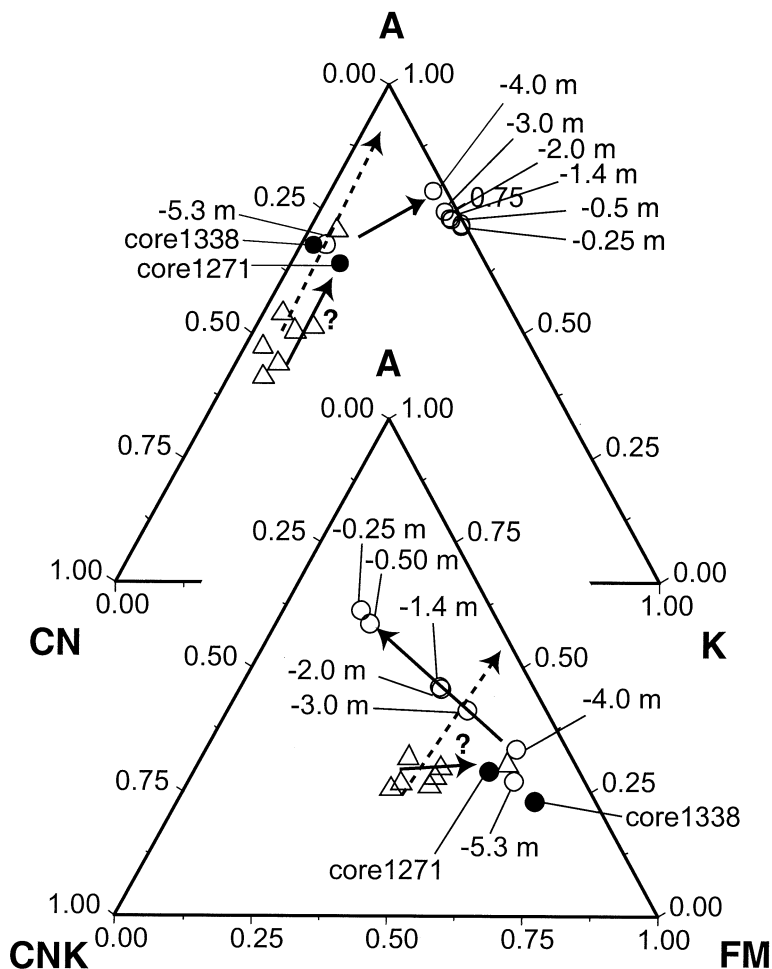


Fig. 10. A-CN-K and A-CN-K-FM ternary diagrams. A, CN, and K, represent the molar proportions of Al, Ca + Na, and K, respectively, and A, CNK, and FM represent the molar proportions of Al, Ca + Na + K, and Fe + Mg, respectively. Circles are data for the present study. For comparison, the data of fresh basalt (Macfarlane et al., 1994) are plotted (open triangles). The solid lines represent possible trends for the present study and the dotted lines possible modern weathering trends (Nesbitt, 1992).

supported by the Science Grant of the Ministry of Education, Science and Culture.

Associate editor: L. Kump

REFERENCES

- Bennett G., Card K. D., Tomlinson K. Y. (1997) The Huronian Supergroup between Sault Ste. Marie and Elliot Lake, Evidence for the early Proterozoic atmosphere, climate and tectonics. Institute on Lake Superior Geology, 43rd annual meeting, May 6–11, Sudbury, Ontario, Field trip Guidebook, 43, part 2, p.76.
- Braun J.-J., Pagel M., Muller J.-J., Bilong P., Michard A., and Guillet B. (1990) Cerium anomaly in lateritic profiles. *Geochim. Cosmochim. Acta* **54**, 781–795.
- Braun J.-J., Pagel M., Herbillon A., and Rosin C. (1993) Mobilization and redistribution of REEs and thorium in a syenitic lateritic profile: A mass balance study. *Geochim. Cosmochim. Acta* **57**, 4419–4434.
- Card K. D. (1978) *Geology of the Sudbury-Manitowlin area, districts of Sudbury and Manitowlin*. Ontario Geological Survey, Report 166, p. 238.
- Fedo C. M., Nesbitt H. W., and Young G. M. (1995) Unraveling the effects of potassium metasomatism in sedimentary rocks and paleosols, with implications for paleoweathering conditions and provenance. *Geology* **23**, 921–924.
- G.-Farrow C. E. and Mossman D. J. (1988) Geology of Precambrian paleosols at the base of the Huronian supergroup, Elliot lake, Ontario, Canada. *Precambrian Res.* **42**, 107–139.
- Harnois L. (1988) The CIW index: A new chemical index of weathering. *Sediment. Geol.* **55**, 319–322.
- Holland H. D. (1984) *The chemical evolution of the atmosphere and oceans*. In *Princeton Series in Geochemistry*, p. 582. Princeton University Press, Princeton, NJ.
- Holland H. D. and Zbinden E. A. (1988) Paleosols and the evolution of the atmosphere. Part I. In *Physical and chemical weathering in geochemical cycles* (eds. A. Lerman and M. Meybeck), pp. 61–82. Kluwer Academic Publishers, Boston.
- Holland H. D. and Beukes N. J. (1990) A paleo-weathering profile from Griqualand west, South Africa: Evidence for a dramatic rise in atmospheric oxygen between 2.2 and 1.9 bybp. *Am. J. Sci.* **290A**, 1–34.
- Holland H. D., Feakes C. R., and Zbinden E. A. (1989) The Flin Flon paleosol and the composition of the atmosphere 1.8 by BP. *Am. J. Sci.* **289**, 362–389.
- Holland H. D. and Rye R. (1997) Evidence in pre-2.2 Ga paleosols for the early evolution of atmospheric oxygen and terrestrial biota: Comment. *Geology* **25**, 857–858.

- Kasting J. F. (1987) Theoretical constraints on oxygen and carbon dioxide concentrations in the Precambrian atmosphere. *Precambrian Res.* **34**, 205–229.
- Kasting J. F. (1991) Box models for the evolution of atmospheric oxygen: An update. *Palaeogeogr. Palaeoclimatol.* **97**, 125–131.
- Kasting J. F. (1993) Earth's early atmosphere. *Science* **259**, 920–926.
- Kasting J. F. and Ackerman T. P. (1986) Climate consequences of very high carbon dioxide levels in the Earth's early atmosphere. *Science* **234**, 1383–1385.
- Krogh T. E., Davis D. W., Corfu F. (1984) Precise U-Pb zircon and baddeleyite ages for the Sudbury area. In *Geology and Ore Deposits of the Sudbury Structure*. (ed. E. G. Pye, A. J. Naldrett, and P. E. Giblin), pp. 431–446, Ontario Geological Survey, Special Vol. 1.
- Macfarlane A. W., Danielson A., and Holland H. D. (1994) Geology and major and trace element chemistry of late Archean weathering profiles in the Fortescue Group, western Australia: Implications for atmospheric P_{CO2}. *Precambrian Res.* **65**, 297–317.
- Middelburg J. J., Van der Weijden C. H., and Woittiez J. R. W. (1988) Chemical processes affecting the mobility of major, minor and trace elements during weathering of granitic rocks. *Chem. Geol.* **68**, 253–273.
- Murakami T., Utsunomiya S., Imazu Y., and Prasad N. (2001) Direct evidence of late Archean to early Proterozoic anoxic atmosphere from a product of 2.5 Ga old weathering. *Earth Planet. Sci. Lett.* **184**, 523–528.
- Nesbitt H. W. (1979) Mobility and fractionation of rare earth elements during weathering of a granodiorite. *Nature* **279**, 206–210.
- Nesbitt H. W. (1992) Diagenesis and metasomatism of weathering profile, with emphasis on Precambrian paleosols. In *Weathering, Soils & Paleosols* (eds. I. P. Martini and W. Chesworth), pp. 127–152. Elsevier, New York.
- Nesbitt H. W. and Young G. M. (1982) Early Proterozoic climates and plate motions inferred from major element chemistry of lites. *Nature* **299**, 715–717.
- Nesbitt H. W., Markovics G., and Price R. C. (1980) Chemical processes affecting alkalis and alkaline earths during continental weathering. *Geochim. Cosmochim. Acta* **44**, 1659–1666.
- Ohmoto H. (1996) Evidence in pre-2.2 Ga paleosols for the early evolution of atmospheric oxygen and terrestrial biota. *Geology* **24**, 1135–1138.
- Ohmoto H. (1997) Evidence in pre-2.2 Ga paleosols for the early evolution of atmospheric oxygen and terrestrial biota: Reply. *Geology* **25**, 858–856.
- Palme H., Suess H., and Zeh H. D. (1981) *Abundances of the elements in the solar system*. In *Landolt-Bornstein Vol. 2a (Astronomy and Astrophysics)*, pp. 257–272. Springer-Verlag, Berlin.
- Pinto J. P., Holland H. D. (1988) Paleosols and the evolution of the atmosphere; Part II. Geological Society of America Special Paper. **216**, pp. 21–34.
- Prasad N., Roscoe S. M. (1991) Profiles of altered zones at ca. 2.45 Ga unconformities beneath Huronian strata, Elliot Lake, Ontario: Evidence for early Archean weathering under anoxic conditions. In *Current Research, Part C*. Geological Survey of Canada, Paper 91-1C, pp. 43–54.
- Prasad N. and Roscoe S. M. (1996) Evidence of anoxic to oxic atmosphere change during 2.45–2.22 Ga from lower and upper sub-Huronian paleosols, Canada. *Catena* **27**, 105–121.
- Prasad N., Robertson J. A., Bennett G. (1993) Paleoweathering, paleosurfaces and Precambrian stratigraphy, Elliot Lake - Thessalon area. IGCP 317, Fourth Meeting—Symposium on Paleoweathering and Paleolandforms. Third International Geomorphology Conference, Hamilton, Ontario, August 23–29, 1993. Guidbook, p. 69.
- Rainbird R. H., Nesbitt H. W., and Donaldson J. A. (1990) Formation and diagenesis of a sub-Huronian saprolite: Comparison with a modern weathering profile. *J. Geol.* **98**, 801–822.
- Robertson J. A. (1970) Geology of the Spragge area. Geological report 76, Ontario Department of Mines, p. 109.
- Robertson J. A. (1981) The uranium deposits of Ontario - Their distribution and classification. Ontario Geological Survey Miscellaneous Paper 86, p. 37.
- Rye R. and Holland H. D. (1998) Paleosols and the evolution of atmospheric oxygen: A critical review. *Am. J. Sci.* **298**, 621–672.
- Rye R., Kuo P. H., and Holland H. D. (1995) Atmospheric carbon dioxide concentrations before 2.2 billion years ago. *Nature* **378**, 603–605.
- Sutton S. J. and Maynard J. B. (1993) Sediment- and basalt-hosted regoliths in the Huronian supergroup: Role of parent lithology in middle Precambrian weathering profiles. *Can. J. Earth Sci.* **30**, 60–76.
- Yoshida H. and Takahashi N. (1997) Chemical behavior of major and trace elements in the Horoman mantle diapir, Hidaka belt, Hokkaido, Japan (in Japanese with English abstract). *J. Mineral. Petrol. Econ. Geol.* **92**, 391–409.